

# Engineering Notes

ENGINEERING NOTES are short manuscripts describing new developments or important results of a preliminary nature. These Notes should not exceed 2500 words (where a figure or table counts as 200 words). Following informal review by the Editors, they may be published within a few months of the date of receipt. Style requirements are the same as for regular contributions (see inside back cover).

## Examining Groundtrack Geometry Transitions by Evaluating the Number of Longitude-Rate Zeros

Justin L. R. Langlois\*

United States Navy, University of Michigan, Ann Arbor,  
Michigan 48109-2140

and

Daniel Scheeres†

University of Colorado, Boulder, Colorado 80309-0429

DOI: 10.2514/1.34089

### Introduction

THE mission of an Earth observation satellite is closely linked to its groundtrack, the projection of its orbit onto the surface of the Earth. Previous work has evaluated examples of useful groundtracks (Molniya, geosynchronous, repeating groundtracks, etc.), their applications, and performing orbit maintenance to sustain these orbits [1,2]. Although there are resources that explain the general groundtrack variations that result from changing orbital elements, there has been little systematic study of these variations [3].

The research presented in this paper addresses this problem by analyzing some simple properties of groundtrack geometry. Specifically, solving for zero values in the speed of the groundtrack in the longitude, or east–west direction, is examined. This analysis is important because reversals in longitude help define the possible shapes of a groundtrack over an orbit period. This paper will outline the method used in solving this problem, including the relevant two-body orbit groundtrack equations, the method used to find the zero values, the method of analysis, and the results of the analysis.

### Theory

#### Orbit Equations

For the two-body problem, the orbital elements of a spacecraft can be used to write the vector of the spacecraft's position and velocity in terms of a Cartesian  $XYZ$  frame fixed in the Earth. The  $XYZ$  frame has its origin at the Earth's center, where the  $X$  axis is in the equatorial plane of the Earth and points toward the prime meridian, and the  $Z$  axis goes through the true north pole of the Earth. The representation of the position unit vector with respect to the orbital elements is given as

$$\begin{aligned} \hat{\mathbf{r}} = & [\cos(w + v) \cos \Omega_B - \sin(w + v) \sin \Omega_B \cos i] \hat{\mathbf{x}} \\ & + [\cos(w + v) \sin \Omega_B + \sin(w + v) \cos \Omega_B \cos i] \hat{\mathbf{y}} \\ & + [\sin(w + v) \sin i] \hat{\mathbf{z}} \end{aligned} \quad (1)$$

where

$w$  = argument of perigee       $v$  = true anomaly

$\Omega_B = \Omega_0 - \dot{\theta}_E(t - t_0)$  = Earth-fixed longitude of ascending node

$\Omega_0$  = longitude at  $t_0$        $\dot{\theta}_E$  = rotational rate of the Earth

$i$  = inclination

To determine the angular velocity rates of the groundtrack, one computes the time derivative of the position unit vector. This is simple because the only time-varying terms of the expression are true anomaly and the ascending node term, ignoring perturbations. The time derivative of the longitude of the ascending node is simply the negative of the rotation rate of the Earth. The time derivative of the true anomaly equals

$$\dot{v} = \sqrt{\frac{\mu}{p^3}} (1 + e \cos v)^2 \quad (2)$$

where

$\mu$  = gravitational parameter of the Earth

$p$  = semilatus parameter       $e$  = eccentricity

The position unit vector two-body problem can also be written in terms of latitude and longitude.

$$\hat{\mathbf{r}} = [\cos \delta \cos L] \hat{\mathbf{x}} + [\cos \delta \sin L] \hat{\mathbf{y}} + [\sin \delta] \hat{\mathbf{z}} \quad (3)$$

where

$L$  = longitude       $\delta$  = latitude

The relationships for latitude and longitude with respect to the orbital elements can be found by comparing Eqs. (1) and (3), and are

$$\tan L = \frac{y_B}{x_B} = \frac{\tan \Omega_B + \tan(w + v) \cos i}{1 - \tan(w + v) \tan \Omega_B \cos i} \quad (4)$$

$$\sin \delta = \sin i \sin(w + v) \quad (5)$$

The longitude relationship can be simplified to

$$\tan(L - \Omega_B) = \tan(w + v) \cos i \quad (6)$$

The rates of the longitude and latitude are

$$\dot{L} = \frac{\dot{v} \cos i}{\cos^2 \delta} - \dot{\theta}_E \quad (7)$$

$$\dot{\delta} = \frac{\dot{v} \cos(w + v) \sin i}{\cos \delta} \quad (8)$$

The latitude rate always has two zeros per orbit, except for two special cases. The zeros occur when the latitude is equal to the

Received 17 August 2007; revision received 5 February 2008; accepted for publication 21 February 2008. Copyright © 2008 by the American Institute of Aeronautics and Astronautics, Inc. All rights reserved. Copies of this paper may be made for personal or internal use, on condition that the copier pay the \$10.00 per-copy fee to the Copyright Clearance Center, Inc., 222 Rosewood Drive, Danvers, MA 01923; include the code 0731-5090/08 \$10.00 in correspondence with the CCC.

\*Ensign, Graduate Student, Department of Aerospace Engineering.

†A. Richard Seebass Chair, Department of Aerospace Engineering Sciences, Associate Fellow AIAA.

inclination above and below the equator with exceptions for inclinations of 0 and 90 deg.

In contrast, the zeros of the longitude rate are not intuitive. Zeros of the longitude rate correspond to points in the orbit where the spacecraft's angular rate in longitude equals the Earth's rotational rate. The number of zero crossings in longitude can influence the shape of the groundtrack and can be used as a design parameter. We show that such crossings can occur up to four times per orbit and describe the number of zero crossings as a function of orbital elements. In the next section, the method of manipulating the longitude-rate equation will be presented.

### Longitude-Rate Equation

To find the zeros of the longitude rate, Eq. (7) is first written using only orbital elements, resulting in

$$\dot{L} = \sqrt{\frac{\mu}{p^3}} \frac{(1 + e \cos v)^2 \cos i}{1 - \sin^2 i \sin^2(w + v)} - \dot{\theta}_E \quad (9)$$

Setting the longitude rate equal to zero, the following relationship exists:

$$\frac{(1 + e \cos v)^2 \cos i}{1 - \sin^2 i \sin^2(w + v)} = \dot{\theta}_E \sqrt{\frac{p^3}{\mu}} = N \quad (10)$$

where  $N$  is constant in the unperturbed problem. Using trigonometric identities and setting  $x = \cos v$ , a second-order equation can be derived in terms of  $x$ .

$$(1 + ex)^2 \cos i - N + x^2 N \sin^2 i \sin^2 w + N \sin^2 i \cos^2 w (1 - x^2) = -2x N \sin^2 i \sin w \cos w \sin v \quad (11)$$

At this point, the equation is second order in  $x$  but also contains a term  $\sin v = \pm \sqrt{1 - x^2}$ . We note that the solutions to this equation will have a definite sign for the term  $\sin v$ , and that both values cannot solve the system. However, to get a polynomial equation with only cosines of the true anomaly, both sides of the equation are squared to created a fourth-order equation.

$$[(1 + ex)^2 \cos i - N + x^2 N \sin^2 i \sin^2 w + N \sin^2 i \cos^2 w (1 - x^2)]^2 = 4x^2 N^2 \sin^4 i \sin^2 w \cos^2 w (1 - x^2) \quad (12)$$

Although the cosine function is symmetric and has two solutions for each value between  $-1$  and  $1$ , this is only an artifact of the squaring step of the preceding derivation. Therefore, there is only one true solution or longitude-rate zero for each root of the polynomial [cf. Eq. (11)].

After simplification, the fourth-order polynomial can be written as

$$Ax^4 + Bx^3 + Cx^2 + Dx + E = 0 \quad (13)$$

where

$$\begin{aligned} A &= -\sin^4 i N^2 + 2e^2 \cos i \sin^2 i \cos(2w)N - e^4 \cos^2 i \\ B &= 4e \cos i [N \sin^2 i \cos(2w) - e^2 \cos i] \\ C &= 2\sin^2 i [\sin^2 w - \cos^2 i \cos^2 w] N^2 + 2 \cos i [\sin^2 i \cos(2w) \\ &\quad + (1 - \sin^2 i \cos^2 w) e^2] N - 6e^2 \cos^2 i \\ D &= 4e \cos i [N(1 - \sin^2 i \cos^2 w) - \cos i] \\ E &= -[N(1 - \sin^2 i \cos^2 w) - \cos i]^2 \end{aligned}$$

We will study the properties of the solutions to this polynomial using the quartic equation techniques explained further in the next section. We note that the coefficients of the polynomial are functions of only four parameters ( $N, e, i, w$ ).

### Method of Analyzing the Fourth-Order Equation

Using Ferrari's method, the discriminant of the equation  $\Delta$  can be computed [4].

$$\Delta = -4P^3 - 27Q^2 \quad (14)$$

where

$$\begin{aligned} P &= BD - 4AE - C^2/3 \\ Q &= -B^2E + BCD/3 + (8/3)ACE - AD^2 - (2/27)C^3 \end{aligned}$$

Using the discriminant, one can make the following assessments:

- 1) For  $\Delta < 0$ , there are two real and two imaginary roots.
- 2) For  $\Delta = 0$ , there are at least two equal real roots.

For a discriminant greater than zero, further discrimination of the roots can be made using Descartes's solution of a quartic equation [4]. Define the new quantities

$$\begin{aligned} \alpha &= 8AC - 3B^2 \\ \beta &= 16A^2(4AE - BD - C^2) - B^2(3B^2 - 16AC) \end{aligned}$$

With these new definitions, we can make the following assessments for a discriminant greater than zero:

- 3) If  $\alpha$  and  $\beta$  are both less than zero, then there are four distinct real roots.
- 4) Otherwise, there are no real roots.

Using MATLAB, a code was generated to organize a graphical presentation of these criteria showing the number of real solutions for the four variables of  $N, i, e$ , and  $w$ . These results are presented in the next section.

## Results

Before we discuss general cases, we will explain some special case solutions. For zero inclination, there is a transition from zero to two solutions at a certain eccentricity that is defined as a function of  $N$ . This relationship can be derived from Eq. (10) by inserting zero for the inclination, resulting in the following relationship:

$$(1 + e \cos v)^2 = N \quad (15)$$

The relationship for  $e$  is then found by solving for  $e$  and setting  $\cos v = -1$  for  $N \leq 1$  and setting  $\cos v = 1$  equal to one for  $N > 1$  greater than one.

$$e = 1 - \sqrt{N}, \quad N \leq 1 \quad e = \sqrt{N} - 1, \quad N > 1 \quad (16)$$

For inclinations of 90 deg or higher, there are never any solutions.

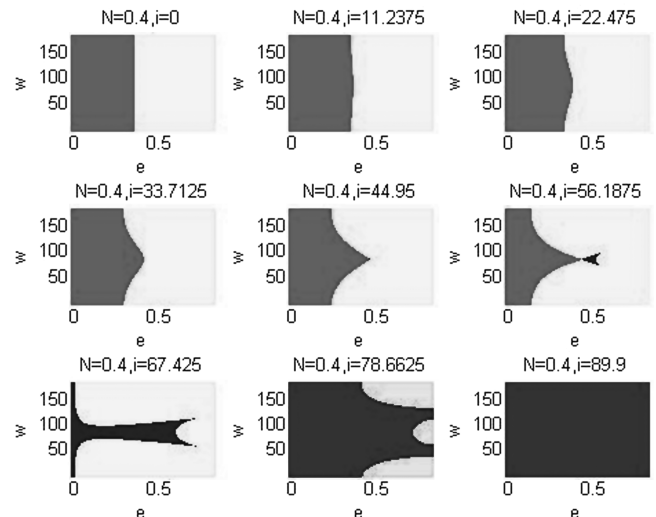


Fig. 1 Real solutions plots for  $N = 0.4$ .

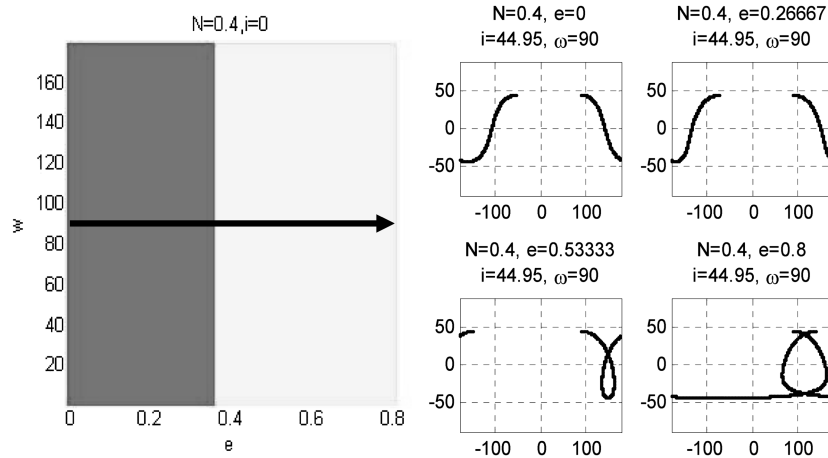


Fig. 2 First transition and associated groundtracks.

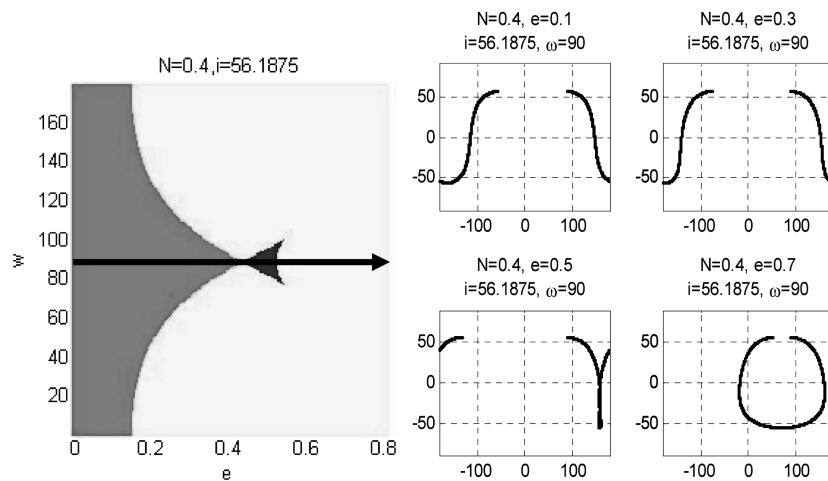


Fig. 3 Third transition and associated groundtracks.

The next special case involves zero eccentricity. At zero eccentricity, there is a transition from zero to four solutions at a certain inclination that is defined as a function of  $N$ . This relationship is also derived from Eq. (10), but zero eccentricity is inserted instead.

$$\frac{\cos i}{1 - \sin^2 i \sin^2(w + v)} = N \quad (17)$$

The relationship for  $i$  is then found by setting  $\sin^2(w + v) = 0$  for  $N \leq 1$  and setting  $\sin^2(w + v) = 1$  for  $N > 1$ .

$$i = \cos^{-1}(N), \quad N \leq 1 \quad i = \cos^{-1}(1/N), \quad N > 1 \quad (18)$$

The final special case discussed is for an  $N$  value of one. An orbit with  $N = 1$  can be described as geosynchronouslike because the semilatus parameter for  $N = 1$  is equal to the geosynchronous distance. For this value of  $N$ , an orbit has two solutions if it has an inclination of zero and a greater than zero eccentricity. Also, an orbit has four solutions if it has zero eccentricity and a greater than zero inclination.

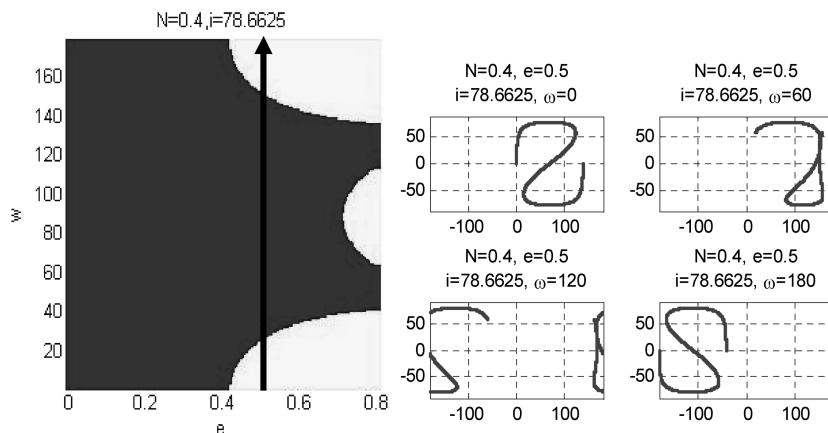


Fig. 4 Further growth of the dark region and associated groundtracks.

All other transitions cannot be explained simply, and so the general case will now be explored. In any case, there are only three transitions: zero to or from two solutions, zero to or from four solutions, and two to or from four solutions. The specific values of elements at which the transitions occur shift with the parameters, but the pattern of transitions remains the same. Note, we only consider cases of  $N < 1$  next. Some differences exist for  $N > 1$  (mainly a 90 deg phase shift with respect to argument of perigee) but are not considered here.

The first set of plots was created for  $w$  and  $e$  for a given  $N$  and  $i$ . In all of the following plots, a region of four real solutions is dark, a region of two real solutions is light, and a region of no real solutions is gray. The repeated roots case is not assigned a color because it is merely the border of the light region. An example of one of these plots is shown in Fig. 1. The graphs are symmetric in terms of argument of perigee, and so  $w$  is shown only for 0–180 deg.

Next, the groundtrack transitions for these plots will be shown. The first transition is from a region of zero solutions to a region of two solutions at zero inclination (Fig. 2). This transition occurs according to Eq. (15).

As inclination is increased, the transition line distorts into a point. The transition from zero to two solutions or vice versa with changing  $w$  is a result of the skewing of the groundtrack. For the third transition, an area of four solutions appears out of the gray point and grows as the inclination increases further (Fig. 3).

This region of four solutions will grow and the area of no solutions will shrink with increasing inclination until the gray region disappears. The graph then only has dark and light regions. The dark region will continue to grow with increasing inclination until the whole graph becomes dark (Fig. 4).

Next, plots were created that placed argument of perigee and inclination on the axes. Similarly, these plots were created for a given value of  $N$  and  $e$ . The graphs of solutions for  $N = 0.5$  is shown in Fig. 5.

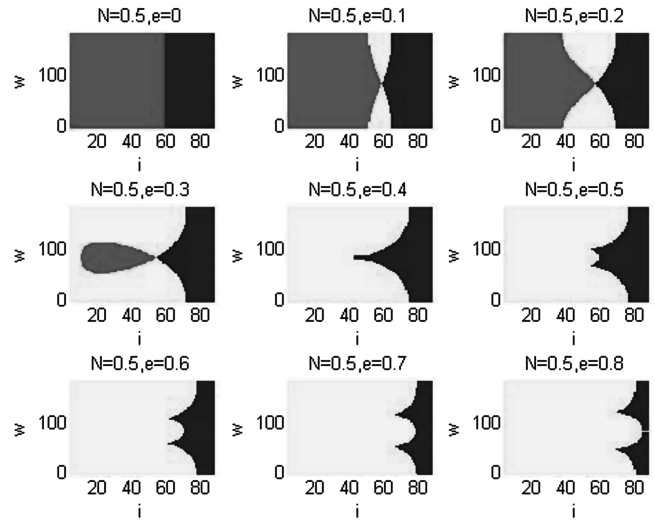


Fig. 5 Real solution plots for  $N = 0.5$ .

Similar to the  $w$ - $e$  plots, the first transition of the  $w$ - $i$  plots involves a straight vertical line that varies its location with the value of  $N$ . However, in the  $w$ - $i$  plots, the transition is from a region of no solutions to a region of four solutions. This transition is given by Eq. (16). The second transition involves the growth of a two solutions region between the gray and dark regions with the gray and dark regions staying connected at  $w = 90$  deg (Fig. 6).

As eccentricity increases, the gray region shrinks until the two solutions region surrounds the zero solutions region (Fig. 7).

The gray region continues to shrink further with increasing eccentricity until the gray region completely disappears (Fig. 8). The

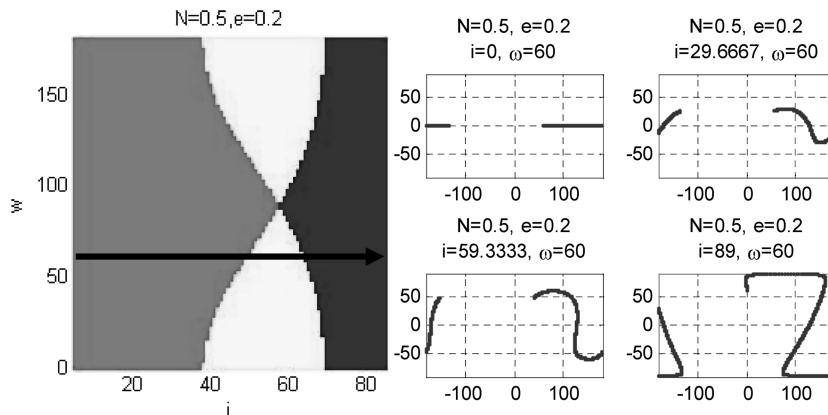


Fig. 6 Second transition and associated groundtracks.

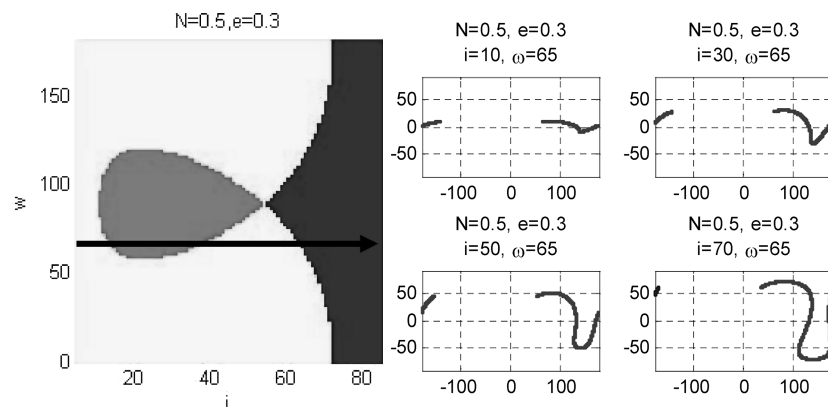


Fig. 7 Third transition and associated groundtracks.

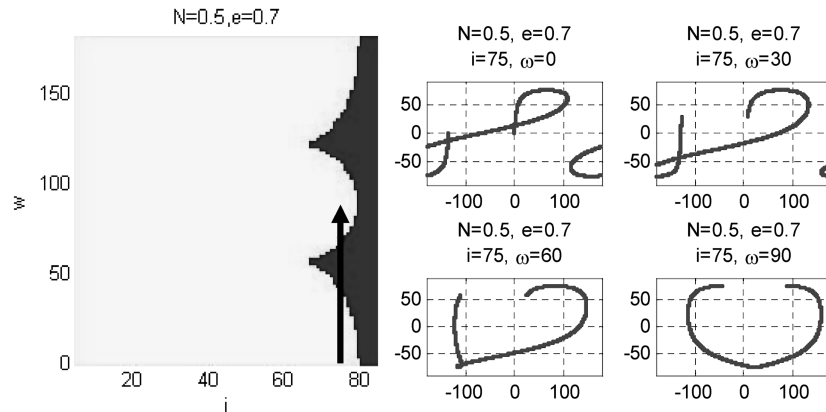


Fig. 8 Fifth transition and associated groundtracks.

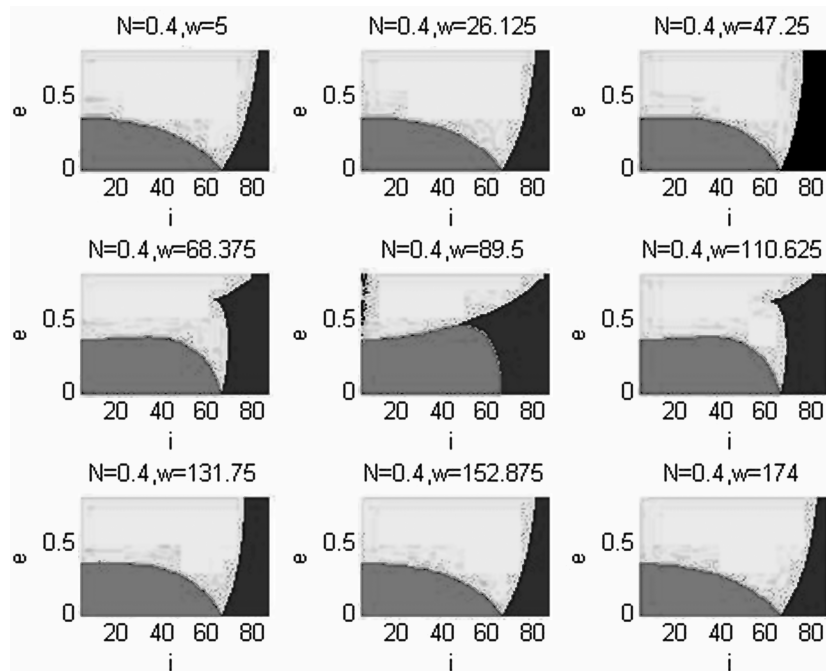


Fig. 9 Real solution plots for  $N = 0.4$  ( $e$  vs  $i$ ).

last transition for increasing eccentricity involves changes in the dark regions. The point of the dark region splits into two points that shift farther apart and toward higher inclination simultaneously, as eccentricity increases further.

To provide a further look at the transitions that occur, Fig. 9 is provided to show the eccentricity vs inclination perspective. These graphs can be compared and verified with the transitions shown in the  $w$ - $e$  and  $w$ - $i$  plots for the same value of  $N$ . The transitions on the axes are given by Eqs. (15) and (16). As  $w$  approaches  $90/270$  deg from either direction, the gray to light to dark transition becomes a gray to dark transition as the light region between them disappears.

### Conclusions

In this research, the issue of groundtrack geometry is approached by analyzing the zeros of longitude rate for Earth orbits. This was accomplished by deriving a fourth-order equation from the longitude-rate equation and examining the properties of the coefficients. By examining the coefficient properties, graphs can be

created with respect to  $N$ ,  $e$ ,  $i$ , and  $w$  that contain regions of zero, two, and four solutions. From these graphs, it is clear that the transitions vary with parameter values but also have a consistent structure. From these known transitions, one can choose a type of groundtrack geometry and use the mathematical relationships provided in this paper to locate regions where those types of groundtrack geometries occur.

### References

- [1] Larson, W. J., and Wertz, J. R., *Space Mission Analysis and Design*, 3rd ed., Microcosm Press, El Segundo, CA, 1999, pp. 137–146.
- [2] Bruccoleri, C., and Mortari, D., *Flower Constellations Visualization and Analysis Tool*, IEEE Publications, Piscataway, NJ, 2005.
- [3] Vallado, D. A., *Fundamentals of Astrodynamics and Applications*, 2nd ed., Microcosm Press, El Segundo, CA, 2001, pp. 126–130.
- [4] Conkwright, N. B., *Introduction to the Theory of Equations*, Ginn, Boston, 1941, pp. 38–42, 42–45.